Supplementary Information (SI) for Materials Horizons.
This journal is © The Royal Society of Chemistry 2025

Supporting Information

Synergistic solid-liquid hybrid electrolyte for cycle-stable and high-efficiency Li-$CuCl_2$ batteries

Qianqian Shen,[ab] Yechao Lin,[ab] Hongge Pan,[ac] Mi Yan,[a] Xuan Zhang,*[ab], Yinzhu Jiang,*[ab]

a School of Materials Science and Engineering, Zhejiang University, Hangzhou, Zhejiang 310027, China

b Future Science Research Institute, ZJU-Hangzhou Global Scientific and Technological Innovation Center, Zhejiang University, Hangzhou, Zhejiang 311215, China

c Institute of Science and Technology for New Energy, Xi'an Technological University, Xi'an, Shanxi 710021, China

*Corresponding author. E-mail: xuanzhangzju@zju.edu.cn; yzjiang@zju.edu.cn

Preparation of cathode

Copper chloride ($CuCl_2$, Aladdin, 98%) and Ketjenblack (KB, Akzo Nobel, Japan) were used as received for the preparation of the active powder. The active powder $CuCl_2$@KB was obtained by high energy ball milling the raw material $CuCl_2$ and KB in a mass ratio of 4:1 for 1 h. All cathodes were made by a traditional slurry-coating method where active powder, KB, and poly(vinylidene fluoride) (PVDF) binder were ground at a mass ratio of 80:10:10 and then homogenized in n-methyl-2-pyrrolidone (NMP) at a speed of 3800 rpm in a micro homogenizer (MSK-SFM-12M) for 9 minutes. The slurry was then bladed on Al foil to render uniform coating, which was further dried in a vacuum oven at 100 °C for 12 h and the active material mass loading was around 0.5-1 mg cm^{-2}. All cathodes were prepared in a completely dry environment.

Preparation of polymer interfacial layer coated solid electrolyte

$Li_{1.5}Al_{0.5}Ge_{1.5}(PO_4)_3$ (LAGP) powder was bought from Hubei Solid New Energy Technology Co., Ltd and pressed as a pellet, then the pellet was calcined at 900 ^oC for 8 h with a heating rate of 5 ^oC min^{-1} to form LAGP pellet. The thickness and paking density of LAGP pellet is 0.95 mm (Fig. S1a) and 3.14 g cm^{-3}, respectively. The LAGP is coated by the polymer interfacial layers. Polymer interfacial layer was prepared by dissolving Poly (vinylidene fluoride-co-hexafluoropropylene) (PVDF-HFP, Macklin), bis(trifluoromethylsulfonyl)imide (LiTFSI, Macklin, 99.9%), and Succinonitrile (SN, Sigma-Aldrich, 99%) in N,N-dimethylformamide (DMF) solvent at a mass ratio of 1:1:0.05 to make a solution. The solid electrolyte was coated by dropping about 10 µL of solution on one side of LAGP and heating at 80 ^oC for 5 h to remove DMF. The thickness of the polymer interfacial layer is 10 µm (Fig. S1b).

Assembly of Li|HE|$CuCl_2$ and Li|8 M|$CuCl_2$ cells

The Li|HE|$CuCl_2$ cells were made with the prepared cathodes, a lithium metal anode, and coated LAGP electrolyte assembling the 2032 coin-type cells in an argon-filled glovebox (<0.01 ppm of H_2O, <0.01 ppm of O_2). Lithium bis(fluorosulfonyl)imide (LiFSI, Macklin, 99%) and dimethoxy ethane (DME, Macklin, 99%) were purchased as raw materials to prepare the liquid electrolyte, which was composed of 8 M LiFSI in DME. 7 μL and 2 μL of liquid electrolyte (8 M LiFSI in DME) were used to wet the positive and negative side interface, respectively. The Li|8 M|$CuCl_2$ cells were assembled with glass fiber (GF/D) as separator and ~180 μL liquid electrolyte was added to assemble the 2025 coin-type cells.

Material characterization

Phase structures of the as-prepared materials were investigated by X-ray diffraction (XRD) on a Bruker D8 diffractometer (equipped with Cu-Kα radiation) with a scan range of 10-80°. Scanning electron microscopy (SEM, Hitachi S-4800) measurements were employed to characterize the morphology and microstructure of samples and electrodes. FTIR was recorded by a NEXUS 670 FTIR instrument. Raman measurements were performed on a Horiba Jobin Yvon Labram Aramis using a 532 nm diode-pumped solid-state laser. X-ray photoelectron spectroscopy (XPS) characterization was carried out on a Thermo Scientific Kalpha spectrometer with mono Al-Kα excitation (1486.6 eV). The copper concentrations in the electrolytes were measured as a function of cycle number *via* ICP-MS (NexION 300X, PerkinElmer). The Vickers hardness s was tested using a microhardness tester (MHVS-50T)

Electrochemical measurements

Electrochemical impedance spectroscopy (EIS) tests of the core-cell batteries were performed on the Autolab electrochemical workstation in a frequency ranging from 1.0 MHz to 0.01 Hz using an amplitude of 50 mV.

Lithium-ion transference number was measured utilizing amperometric technique with an applied DC voltage of 10 mV and EIS measurement in a lithium symmetric cell incorporating hybrid electrolytes as electrolyte. EIS was tested before and after the DC polarization conducted by amperometric technique. The $t_{\mathrm{Li+}}$ value was calculated according to Bruce's equation: $t_{Li+} = I_s (\Delta V - I_0 R_0) / (I_0 (\Delta V - I_s R_s))$, where ΔV was the polarization voltage (10 mV), I_0 was the initial current, I_s was the steady state current, R_0 was the initial resistance, and R_S was the steady state total resistance.

The batteries were charged and discharged between a voltage range of 1.9-4.0 V at 30 ^{o}C. The specific capacity values and current densities were calculated based on the mass of active materials. The galvanostatic intermittent titration technique (GITT) was tested at 20 mA g^{-1}, with each current pulse lasting 60 minutes, and the resting time was 10 h. The cyclic voltammetry (CV) curve was obtained using a CHI660C electrochemical workstation.

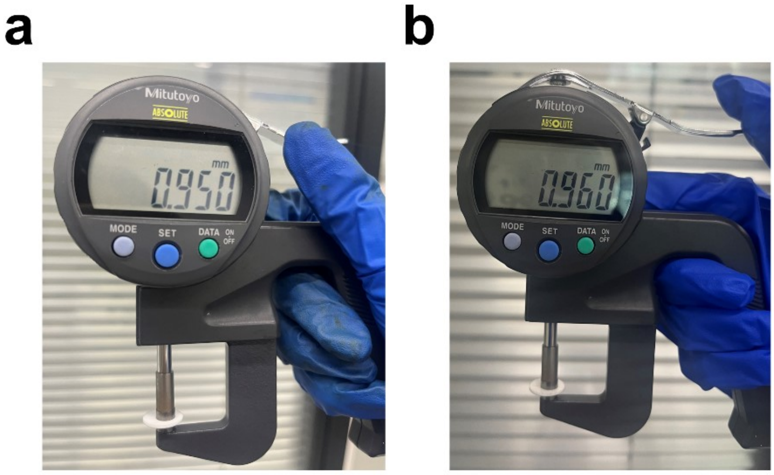

Fig. S1 The thickness of (a) pristine LAGP and (b) the polymer-coated LAGP.

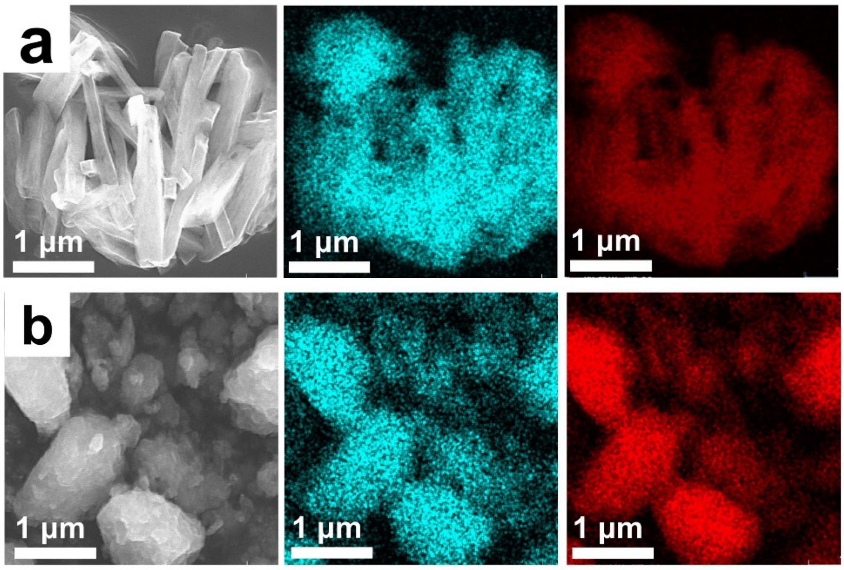

Fig. S2 SEM and EDS images of (a) $CuCl_2$ and (b) $CuCl_2$@KB mixture.

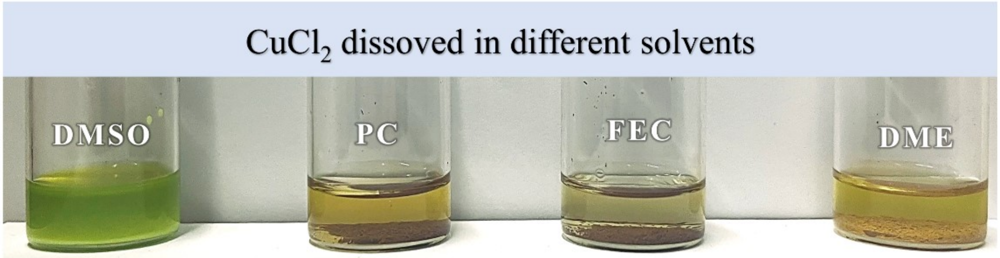

Fig. S3 Optical images of $CuCl_2$ dissolved in various solvents, including dimethyl sulfoxide (DMSO), propylene carbonate (PC), fluoroethylene carbonate (FEC), and dimethoxyethane (DME).

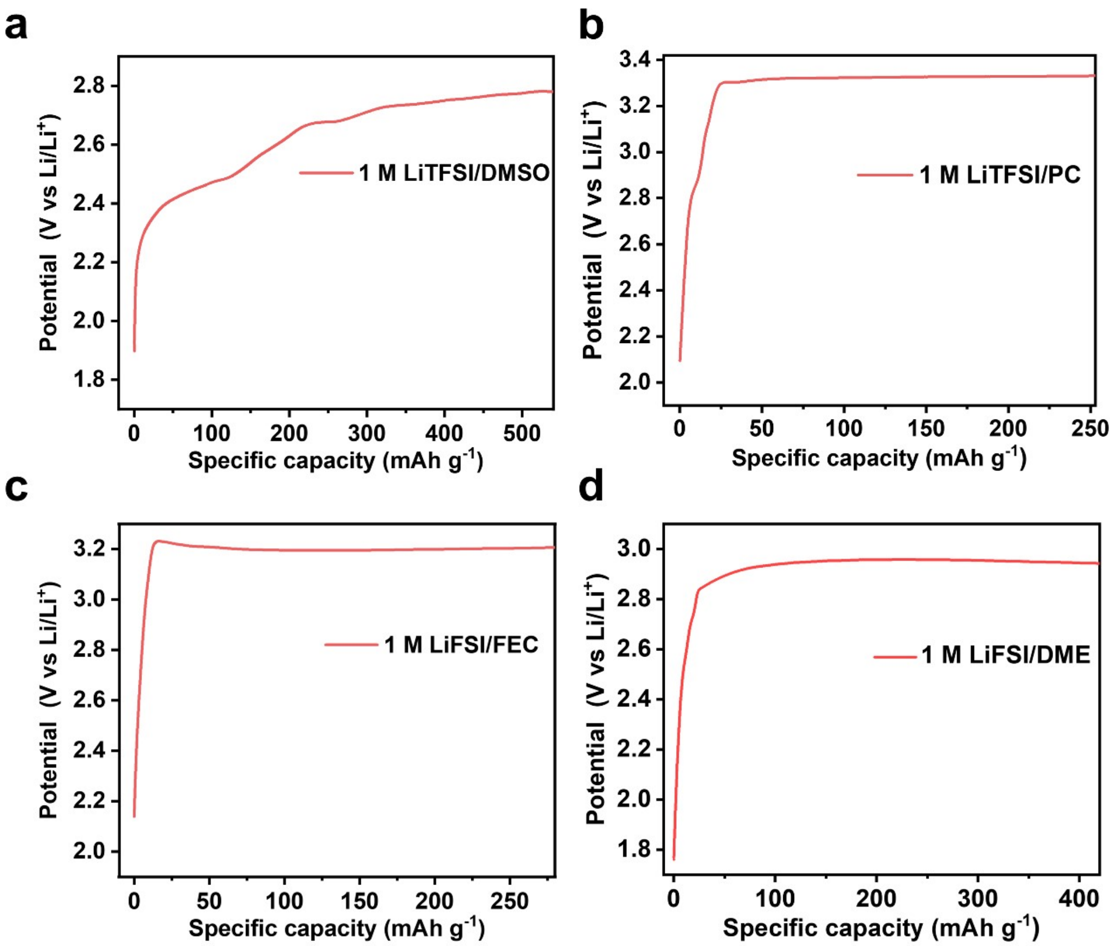

Fig. S4 Charge-discharge profiles of Li-$CuCl_2$ batteries with different electrolytes. (a) 1 M LiTFSI in DMSO. (b) 1 M LiTFSI in PC. (c) 1 M LiFSI in FEC. (d) 1 M LiFSI in DME.

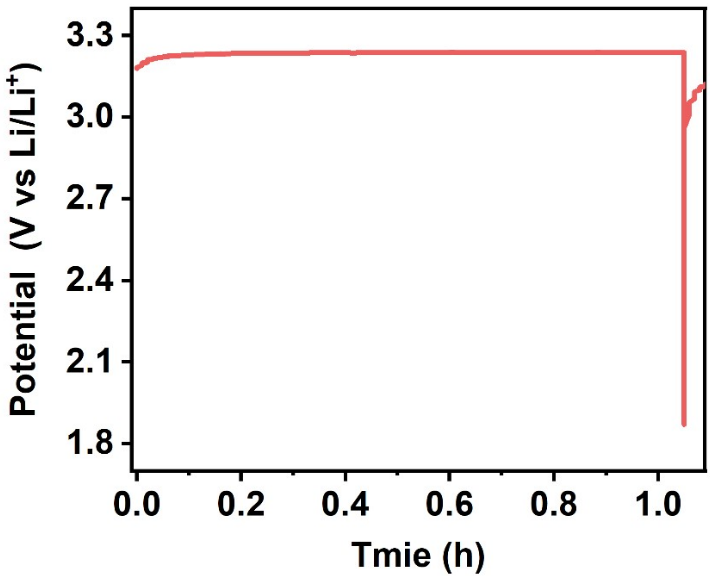

Fig. S5 Charge-discharge profiles of Li-$CuCl_2$ cell with LAGP at 0.05 C

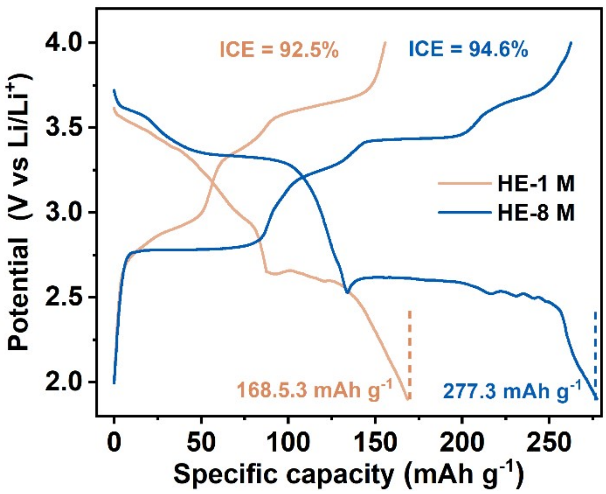

Fig. S6 Charge-discharge profiles of Li-CuCl2 cells with 1 M/8 M LiFSI/DME added in hybrid electrolyte at 0.05 C.

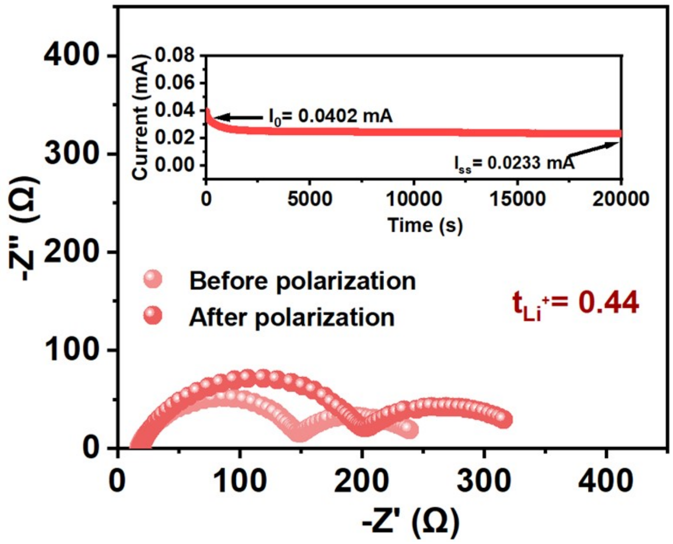

Fig. S7 Nyquist plots of the Li symmetric cell with 8 M LiFSI/DME before and after polarization (the inset is current-time curve at 10 mV polarization).

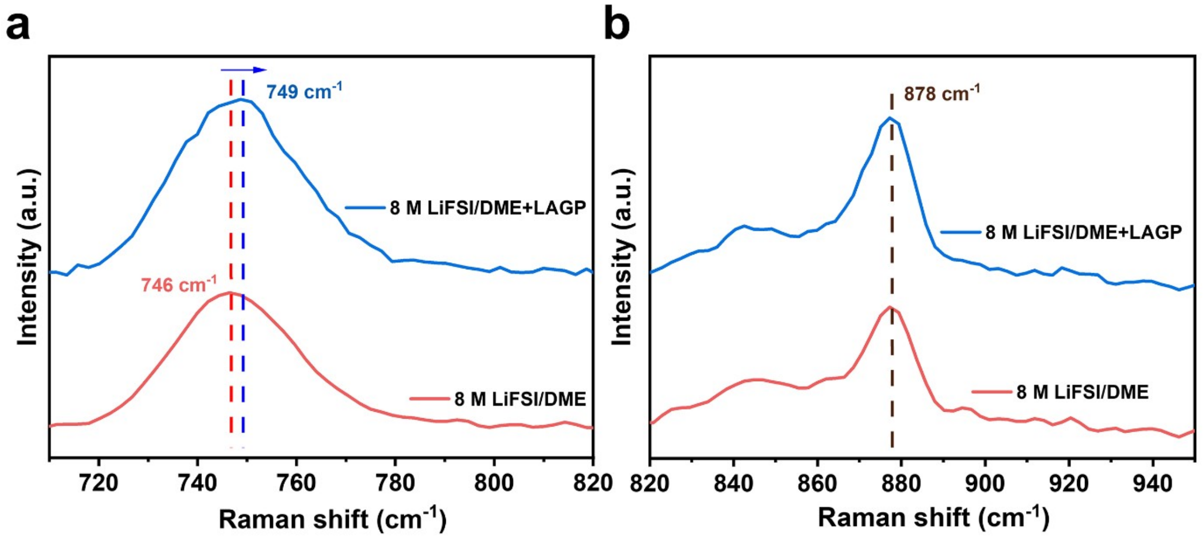

Fig. S8 Comparative Raman spectra of the characteristic peak of (a) FSI^- and (b) DME in 8 M LiFSI/DME baseline electrolyte versus LAGP-containing electrolytes.

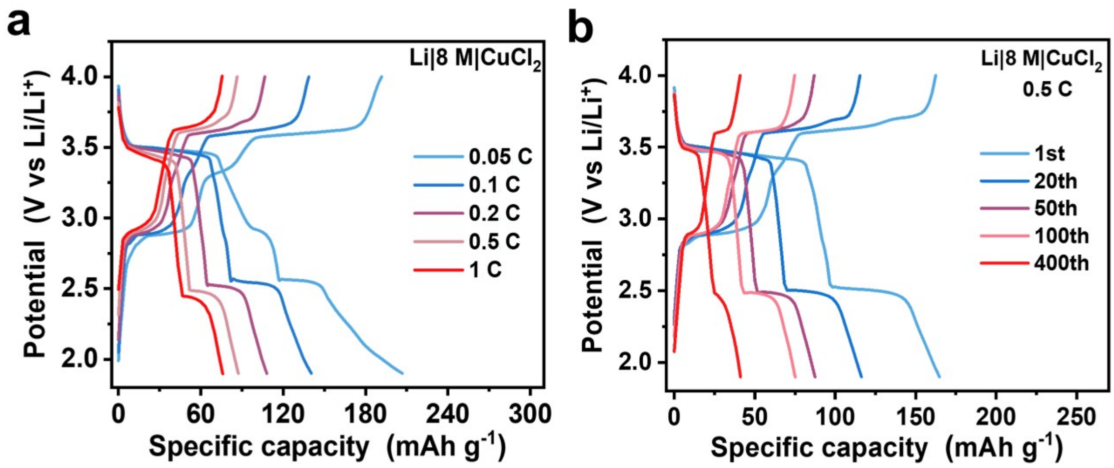

Fig. S9 (a) Rate performance of Li|8 M|$CuCl_2$ cell. **(b)** Charge-discharge curves of the Li|8 M|$CuCl_2$ cell at different cycling stages at 0.5 C.

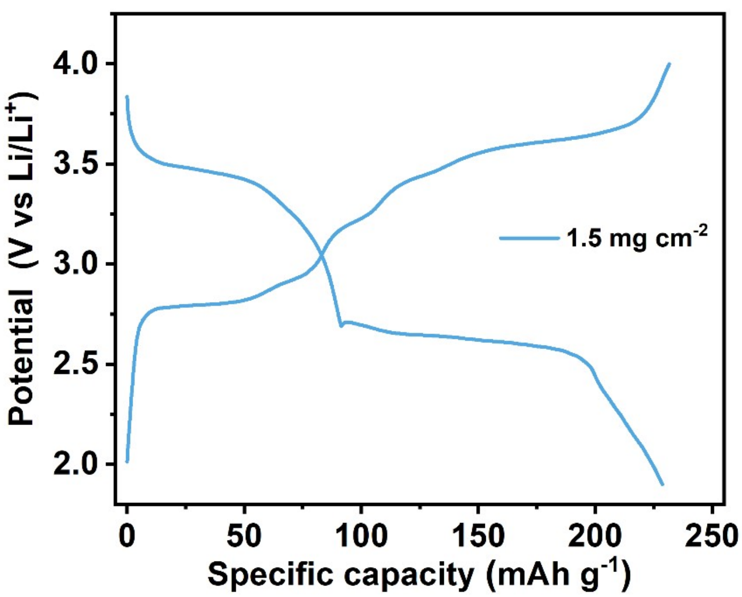

Fig. S10 Galvanostatic chare-discharged profile of Li|HE|$CuCl_2$ cell with higher mass loading.

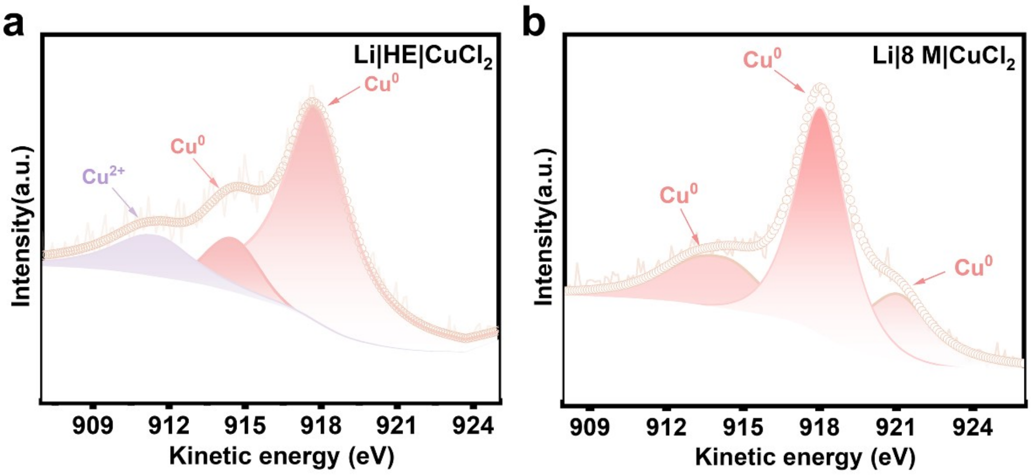

Fig. S11 Cu LMM XPS Auger spectra of $CuCl_2$ cathodes after 100 cycles in (a) HE and (b) 8 M LiFSI/DME system.

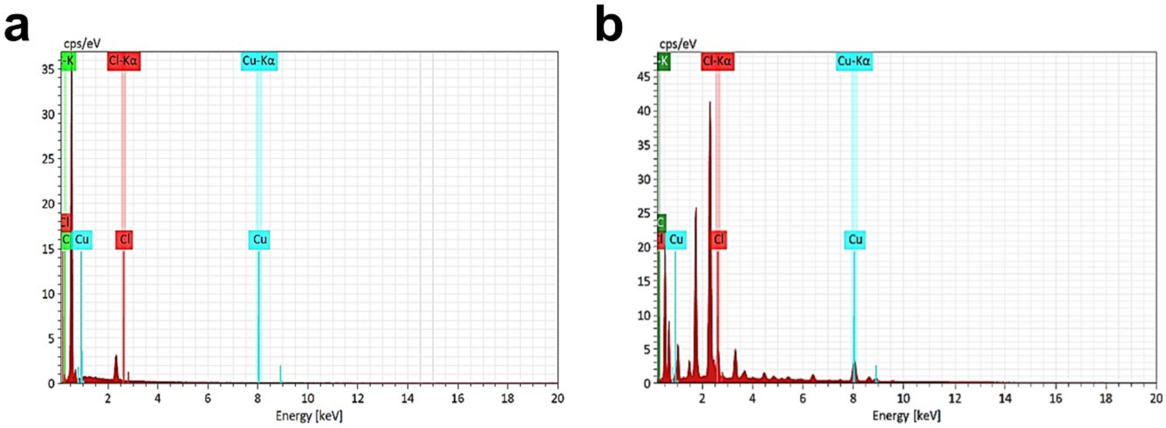

Fig. S12 EDS spectra of anode after 100 cycles in the Li|HE|$CuCl_2$ (a) and (b) Li|8 M|$CuCl_2$ cells.

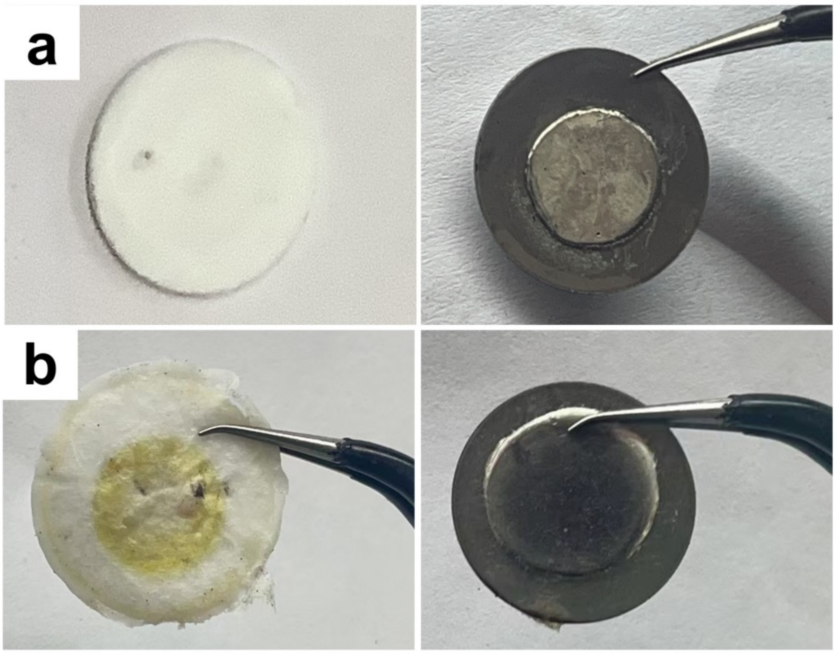

Fig. S13 Photo patterns of the cycled lithium anode and separator in (a) Li|HE|$CuCl_2$ and (b) Li|8 M|$CuCl_2$ cells.

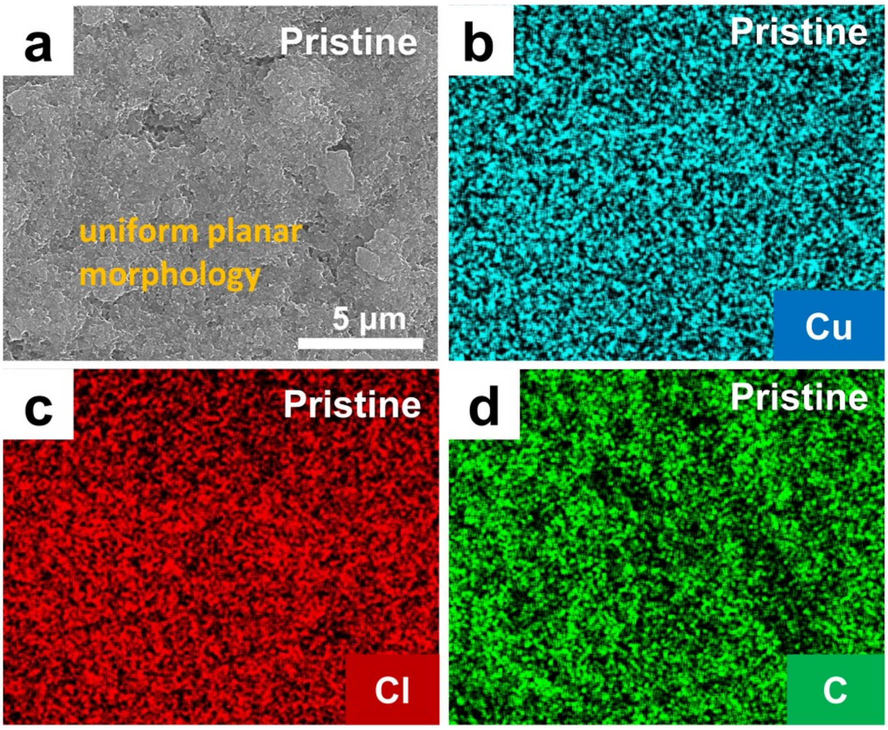

Fig. S14 The SEM images of the (a) pristine $CuCl_2$ cathode and the corresponding EDS mappings of (b) Cu, (c) Cl and (d) C elements.

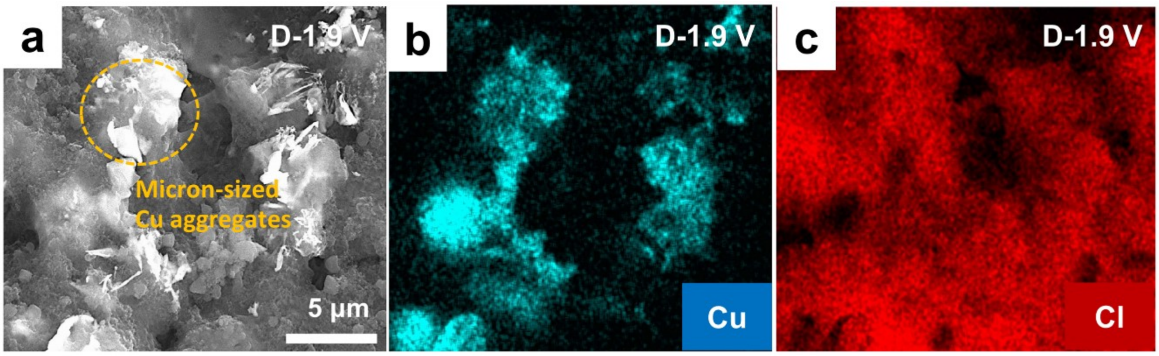

Fig. S15 The SEM images of the (a) discharged $CuCl_2$ cathode and the corresponding EDS mappings of (b) Cu, and (c) Cl elements.

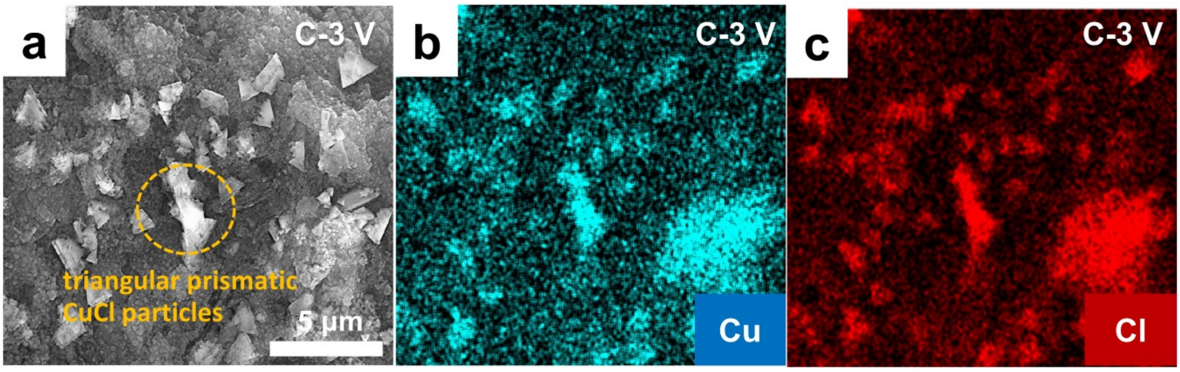

Fig. S16 The SEM images of the (a) charged $CuCl_2$ cathode and the corresponding EDS mappings of (b) Cu and (c) Cl elements.

Table S1. Comparison on the Li^+ transference number (t_{Li+}) between this work and some previous studies of hybrid electrolyte.

System	t_{Li+}	Reference
LATP@SCA-0.25IL	0.40	1
LAGP@IL	0.53	2
t-CSE1	0.69	3
LAGP/SN	0.77	4
SLFE-5%LAGP	0.64	5
LATP@PVDF-co-HFP-LiTFSA/SL	0.64	6
LAGP-8 M LiFS/DME	**0.86**	**This work**

Table S2. Vickers Harness of $CuCl_2$ and LAGP.

Sample	Vickers Harness (Gpa)
$CuCl_2$	0.18
LAGP	8.03

Supplementary references

1. Y. Wu, M. Chao, C. Lu, H. Xu, K. Zeng, D. Li and R. Yang, *Journal of Power Sources*, 2024, **599**, 234206.
2. B. Yan, Y. Qu, H. Ren, X. Lu, Z. Wang, W. Liu, Y. Wang, M. Kotobuki and K. Jiang, *Materials Chemistry and Physics*, 2022, **287**, 126265.
3. D. Y. Kibret, T. H. Mengesha, K. Z. Walle, Y.-S. Wu, J.-K. Chang, R. Jose and C.-C. Yang, *Journal of Energy Storage*, 2024, **94**, 112523.
4. W. Zha, W. Li, Y. Ruan, J. Wang and Z. Wen, *Energy Storage Materials*, 2021, **36**, 171-178.
5. M. Song, C. Tian, T. Huang and A. J. A. A. E. M. Yu, 2023, **6**, 7681-7691.
6. J.-y. Ock, M. Fujishiro, K. Ueno, I. Kawamura, R. Tatara, K. Hashimoto, M. Watanabe and K. Dokko, *ACS omega*, 2021, **6**, 16187-16193.